17th World Conference on Earthquake Engineering, 17WCEE
Sendai, Japan - September 13th to 18th 2020

THE DYNAMIC CHARACTERISTIC CHANGE OF A SKYSCRAPER SKS BUILDING DURING EARTHQUAKES APPLYING THE CERS METHODS

Yutaka Nakamura (1), Jun Saita (2) and Tsutomu Sato (3)

(1) *President, System and Data Research Co., Ltd., Dr. Eng., yutaka@sdr.co.jp*
(2) *Senior Research Engineer, System and Data Research Co., Ltd., jun@sdr.co.jp*
(3) *Senior Research Engineer, System and Data Research Co., Ltd., M. Eng., tsato@sdr.co.jp*

Abstract

During the 2011 off the Pacific coast of Tohoku Earthquake, the SKS building more than 700km far from the epicenter kept shaking with unexpected large amplitude. After this, anti-seismic devices, oil dampers and steel dampers, against resonance were installed individually same kind of damper for each structure direction. This paper investigates the change of the travel time and damping factor in time-series analysis using the CERS methods with opened strong motion records to understand the unexpected resonance and the effect of added anti-seismic devices. As a result, the resonance was caused by drastically decreasing the damping with approaching the input period to the natural period of this building. Here ten earthquakes after installation are also investigated. The damping decreased again at the time of the 2016 Kumamoto earthquake. Oil dampers only contributed to increasing damping as expected, without engaging the stiffness. On the other hand, steel dampers contributed little to increasing damping while contributed to slightly improve the stiffness. It is necessary to keep following the effect of the dampers.

Keywords: CERS methods, Wave Propagation Velocity, Damping, Earthquake, High-rise Building, Anti-seismic Devices

1. Introduction

Many researchers interested in a SKS building of the steel construction with long shaking at the time of the 2011 off the Pacific coast of Tohoku Earthquake occurred at 14:45 JST, March 11, 2011 (hereafter called “311 Earthquake”). This building had been considered installing anti-seismic devices before the 311 Earthquake, and equipped oil dampers and steel dampers in January, 2014. This building was also considered to install additional anti-seismic equipment against estimated huge Nankai trough earthquake. The SKS building had started strong motion observation just before the 311 Earthquake and recorded after the earthquake occurred at March 9, 2011. In this paper, some strong motion records as the 311 Earthquake or the Kumamoto earthquake at April 16, 2016 are analyzed using the CERS methods to make clear the influence of the 311 Earthquake or availability of the anti-seismic devices with tracing the change of the dynamic motion characteristics of the SKS building.

2. Analysis method

First, the CERS methods are briefly explained as follows and please see Nakamura [1, 2] for details.

The CERS methods are an inclusive term of four methods, C, E, R and S methods. The C method calculates in realtime the propagation velocity and damping situation between two points in line on the wave propagation direction in a medium with an end face and a reflecting plane using observed waveform at these two points. The E method computes in realtime the propagation time and damping using a waveform recorded at only one point on the end face or between the end face and the reflecting plane excluding the reflecting plane. The R and S methods are the methods to calculate apparent wave propagation time between two points in realtime. The R method estimates based on maximum correlation between the two observed waveforms and the S method estimates using minimum error. Please see the paper [3] as an example of application for non-linear response of soft layered ground.

Here, the C method is mainly applied. Strong motion is observed at 5 point around the center of the floor at 1F, 18F and 38F and each side of 52F (52FN and 52FS) as Fig. 1. Because the C method supposes that the observed points are roughly lined toward to the direction of wave propagation, here estimates the earthquake motion, 52FC, around the center of the 52F as an average of the both side of 52F and considers a

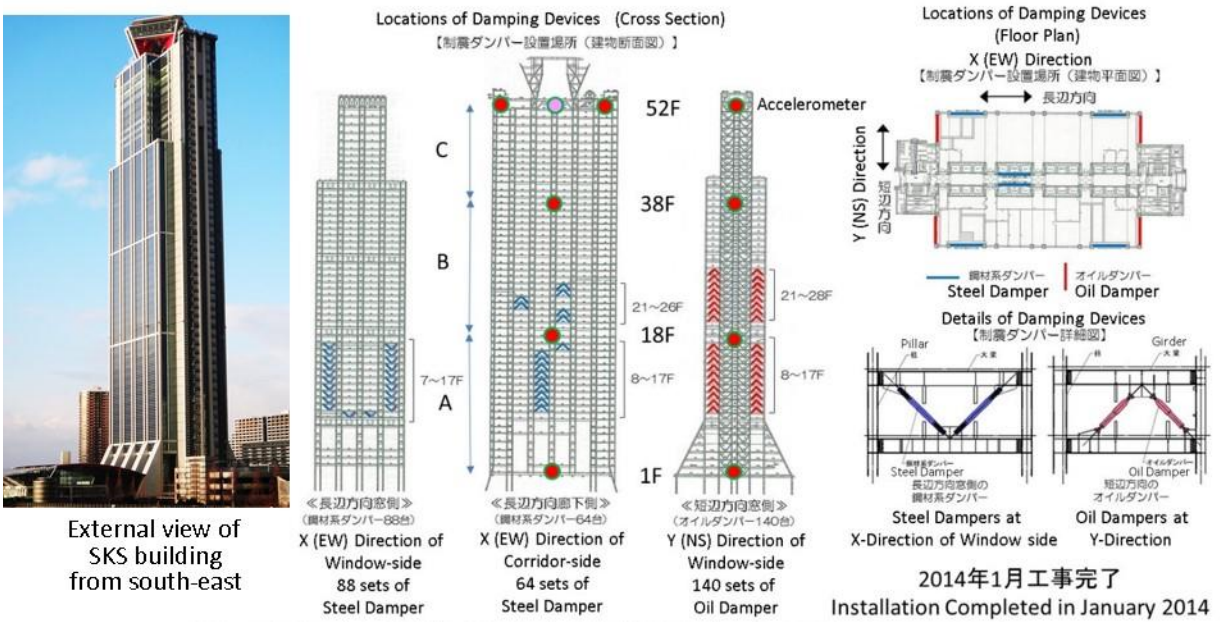

Fig.1 – External view and the locations of accelerometers and damping devices of the SKS building [4]

point on the same vertical line from 1F to 38F.

However, there are abnormal sampling intervals on the opened waveform recorded at 52FN on March 14, 2014 and November 22, 2014, so they are corrected based on the sampling rate of 52FS. The R method is applied to determine the location and degree of the error. This correction caused two lost parts on each waveforms of 52FN. Although these lost parts are filled with the recorded waveform at 52FS, it may cause little affect for analysis because each part is less than one second.

The C method is applied based on 52FC and set target waveform at 38F, 18F and 1F to estimate the wave propagation time and the damping factor between 52FC and each target floor. On the other hand, the E method is applied to the waveform at 1F for the estimation of the wave propagation time and then the natural period of input earthquake motion is assumed as four times of estimated wave propagation time. Here, these C and E methods analysis use strong motion records more than M6 because of little inducement of local short period vibration. The wave propagation time or velocity between each floor is calculated from the analyzed results and the damping factors are also derived. The natural period of the building is calculated as four times of the wave propagation time between 52FC and 1F. Each analysis applies exponential smoothing with half-life period of 40 seconds for averaging. The earthquake motion characteristics of the SKS building is considered with the analysis result above.

3. Analyzed observed earthquake motion at the SKS building and installation condition of additional anti-seismic devices

Table 1 is a list of strong motion records for analysis and Fig. 1 shows the installation condition of additional anti-seismic devices for the SKS building with the locations of the seismometers as a red circle. A pink circle indicates assumed location of 52FC derived from the strong motion records. Based on a document on the earthquake disaster prevention of the SKS building [4], steel dampers and oil dampers were equipped for the long axis (X: EW direction) and the short axis (Y: NS direction), respectively, at the observation period on Table 1. From the viewpoint of the earthquake observation, a figure in the document shows 80 and 64 oil dampers between 1F and 18F (hereafter called “section A”) and between 18F and 38F (hereafter called “section B”), respectively, totally 144 sets but the figure showed 140 sets. Steel dampers have been installed 128 sets for the section A and 24 sets for the section B. This means that the steel dampers have been installed at the X direction mainly for the section A and oil dampers have been installed at the Y direction mainly for both the sections A and B.

Table 1 – List of target events: target of the wave propagation analysis was M>6 events

Eq. No.	SKS	Date	Epicenter	N	E	M	h(km)	Δ (km)	Amax (Gal)	Ijma	Rimax	5HzPGA (Gal)	Length (s)
1	Without	2011/3/9 11:45	Off Sanriku	38.3281	143.2781	7.3	8	813	0	0.4	1.3	0.7	900
2	Damping	2011/3/11 14:46	Off Sanriku	38.1031	142.8600	9	24	769	34	3.0	3.8	15.0	999
3	Devices	2011/3/11 15:15	Off Ibaraki Pref.	36.1081	141.2647	7.6	43	555	9	2.5	3.5	8.9	960
4		2011/3/12 3:59	N Nagano Pref.	36.9850	138.5967	6.7	8	387	1	1.1	1.8	1.6	999
5		2011/3/15 22:31	E Shizuoka Pref.	36.3081	138.5967	6.4	14	309	1	1.3	1.6	1.7	999
6		2011/4/7 23:32	Off Miyagi Pref.	38.2031	141.9197	7.2	66	704	2	1.3	2.0	2.0	960
7		2011/4/11 17:16	Hama-dori, Fukushima Pref.	36.9450	140.6717	7	6	539	1	1.0	1.7	1.4	900
8		2011/7/5 19:18	N Wakayama Pref.	33.9900	135.2331	5.5	7	74	4	1.6	1.7	4.6	720
9		2011/7/10 9:57	Off Sanriku	38.0317	143.5067	7.3	34	816	1	1.0	1.9	1.5	840
10		2011/8/1 23:58	Suruga Bay	34.7081	138.5467	6.2	23	286	1	1.2	1.5	1.9	670
11		2011/10/9 16:18	S Osaka Pref.	34.5031	135.4900	3.9	12	16	5	1.2	1.0	2.5	344
12		2013/4/13 5:33	Near Awaji-shima	34.4181	134.8281	6.3	15	59	23	2.8	2.9	18.6	400
13	With	2014/3/14 2:06	Iyo-nada	33.6917	131.8897	6.2	78	340	1	1.2	1.3	1.5	600
14	Damping	2014/11/22 22:08	N Nagano Pref.	36.6917	137.8897	6.7	5	319	1	1.0	1.7	1.4	600
15	Devices	2015/5/30 20:23	W Off Ogasawara Is.	27.8600	140.6817	8.1	682	904	2	1.3	2.0	1.9	600
16	X: Steel	2016/4/1 11:39	SE Off Mie Pref.	33.3231	136.3817	6.5	29	171	4	2.2	2.5	4.5	600
17	Y: Oil	2016/4/14 21:26	Kumamoto, Kumamoto Pref.	32.7417	130.8081	6.5	11	475	0	0.6	0.9	0.7	600
18		2016/4/15 0:03	Kumamoto, Kumamoto Pref.	32.7000	130.7767	6.4	7	480	0	0.0	0.9	0.5	600
19		2016/4/16 1:25	Kumamoto, Kumamoto Pref.	32.7531	130.7617	7.3	12	478	6	2.4	3.1	6.4	600
20		2016/10/21 14:07	C Tottori Pref.	35.3800	133.8547	6.6	11	164	8	2.5	2.5	8.9	600
21		2016/11/19 11:48	S Wakayama Pref.	33.8417	135.4631	5.4	51	88	4	1.8	1.8	4.4	240
22		2016/11/22 5:59	Off Fukushima Pref.	37.3531	141.6031	7.4	25	633	2	1.6	2.2	2.3	600
23		2017/6/25 7:02	S Nagano Pref.	35.8667	137.5850	5.6	7	239	1	0.7	0.8	1.1	600
24		2018/6/18 7:58	N Osaka Pref.	34.8431	135.6217	6.1	13	29	98	4.0	4.2	81.8	600
25		2018/6/19 0:31	N Osaka Pref.	34.8581	135.6067	4.1	10	30	2	0.3	0.5	1.5	300

4. Change of amplification degree for each section overviewed by realtime seismic intensity RI

Behavior of realtime seismic intensity RI (Nakamura [5]) of each observed floor is derived from the strong motion records at 1F, 18F and 38F, and calculated waveform at 52FC derived from the records. Fig. 2 shows examples of this behavior at the time of the main shock and the largest aftershock of the 311 Earthquake, the main shock of the 2016 Kumamoto earthquake and the Osaka-Fu Hokubu earthquake. Based on this behavior of RI, time variation of intensity amplification is calculated for the section A (between 1F and 18F), the section B (between 18F and 38F) and a section between 38F and 52F (hereafter called "section C"). This analysis was done with distinguishing before and after the installation of the anti-seismic devices. Fig. 3 shows the maximum intensity amplification at the sections between each observation point for each event. From this figure, averaged amplification of the section A was over 0.1/floor before installation and it became less than 0.1/floor and around 0.08/floor almost proportionally to the number of floor after installation. It means that the anti-seismic devices can realize the standardization of amplification degree, so it is noticed as the totally effect of these devices. It is also notable that the amplification degrees of the section A at the time of the largest aftershock of the 311 Earthquake, before installation, and the main shock of the Kumamoto earthquake, after installation, is 0.14 – 0.18/floor far from the degree at the time of the other events. Additionally, it is impressive that the resonance at the time of the main shock of the Kumamoto earthquake, after installation, were occurred at the direction with steel dampers.

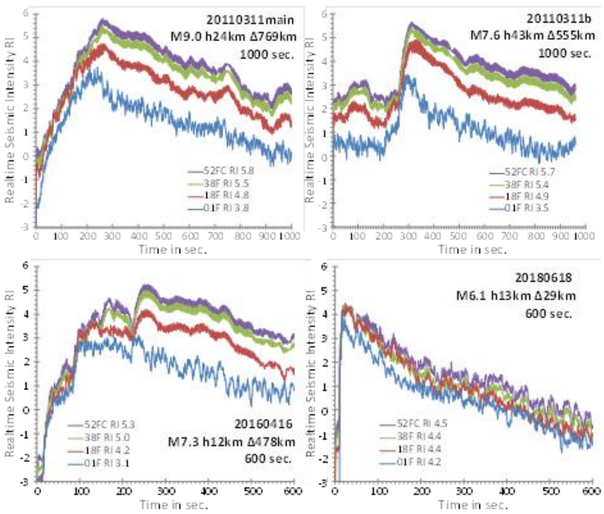

Fig. 2 – Examples of time history change of realtime intensity RI at the floors of observation

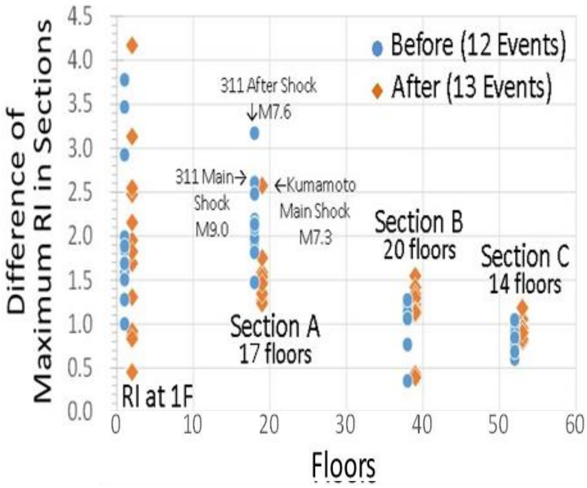

Fig. 3 – Amplification of RI before and after the damping device installation

5. Wave propagation analysis applying the CERS methods

5.1 Result of wave propagation analysis for each event

Fig. 4 summarizes the result of wave propagation analysis with distinguishing the X and Y directions of the building for 20 events, 10 events before installation of the anti-seismic devices and 10 events after installation. Circled number in this figure indicates the assigned number of the earthquake in Table 1, and the occurred date and the earthquake parameters are indicated in upper figure and lower figure under the circled number, respectively. The upper figure shows change of the wave propagation velocity in each section with color-corded as blue for the section C, green for the section B and orange for the section A in m/sec of left axis, and change of the realtime seismic intensity RI at 1F as red and 52FC714s purple in right axis. Because RI is derived from three components, the change of RI is same for both the X and Y components. Here indicates the change of RI at 1F and 52FC, and larger difference of each RI means larger earthquake motion amplification degree of the building. The lower figure shows change of the natural period of the building as

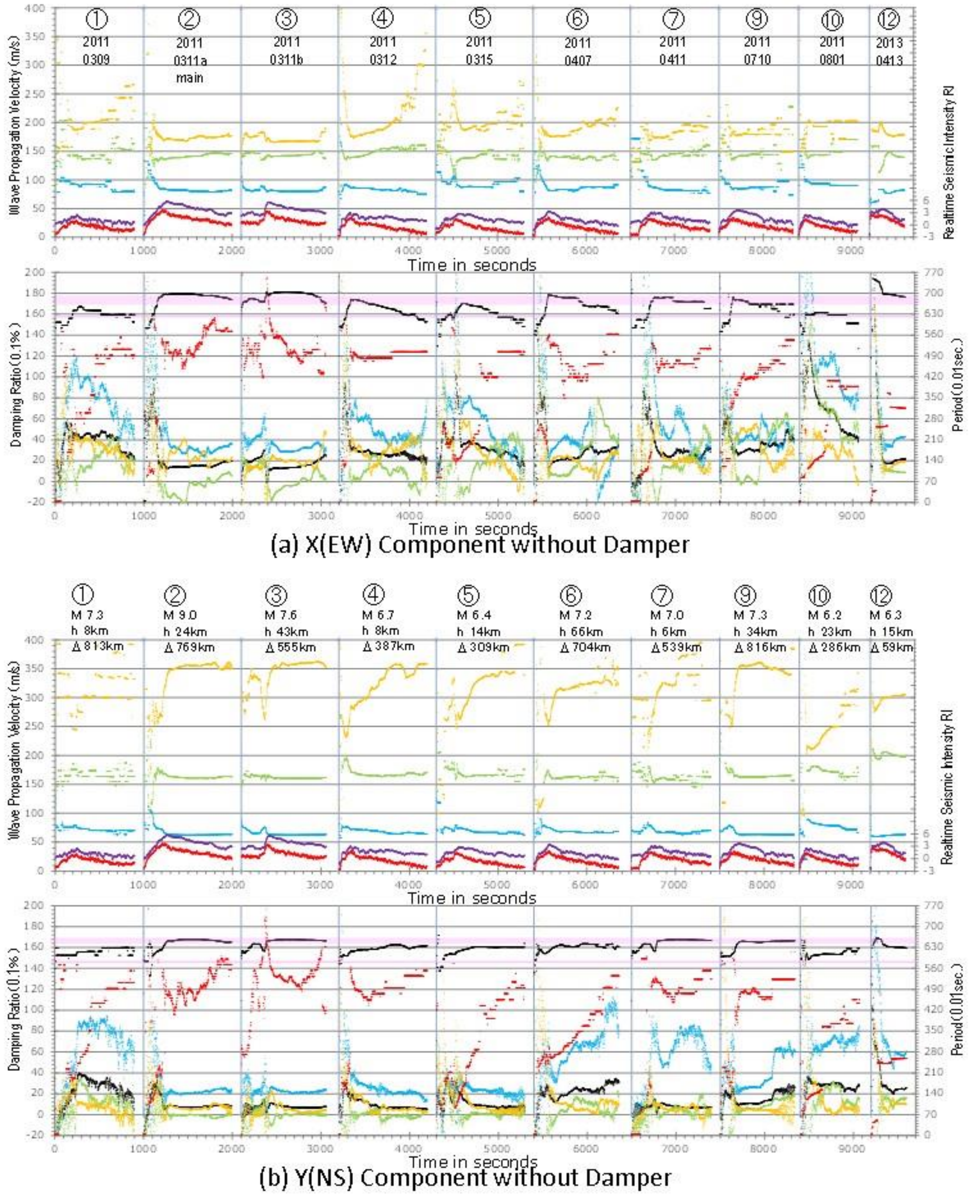

Fig. 4(a)(b) – Results of the travel time analysis before the damper installation; change of the dynamic characteristics of the SKS building

black dots in unit of 1/100 seconds at right axis, change of the natural period of input earthquake motion as red dots in unit of 1/100 seconds at right axis, the damping factor for each section as blue dots for section C, green dots for section B and orange dots for section A in unit of 0.1 % at left axis and the damping factor between 52FC and 1F instead of averaged damping factor for entire the building as black dots in unit of 0.1 % at left axis. Additionally, pink transparent band indicates an area where the natural period of this building exists assessed by the exploratory committee for anti-seismic and transparent line is initial natural period, both in unit of 1/100 seconds at right axis. Horizontal axis in this figure is time scale in second. Also, although the analysis is processed every sampling time of 1/100 seconds, here the result is extracted every 100 samples and indicates every one second. However, the realtime seismic intensity RI indicates the maximum value of every one second. Furthermore, the scale of the wave propagation velocity or the damping factor of each section is same for each event for comparing each other.

5.2 The natural period of the SKS building and entire damping factor

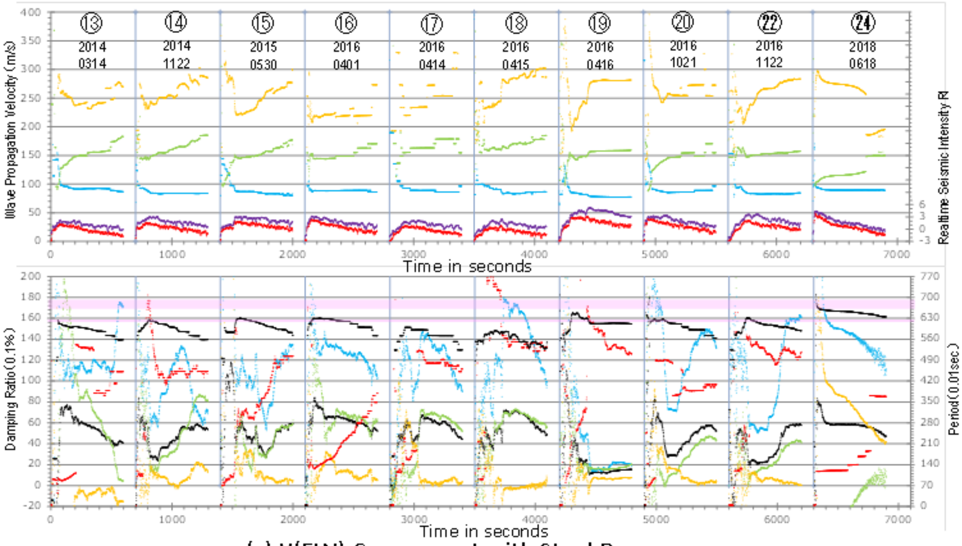

(c) X(EW) Component with Steel Damper

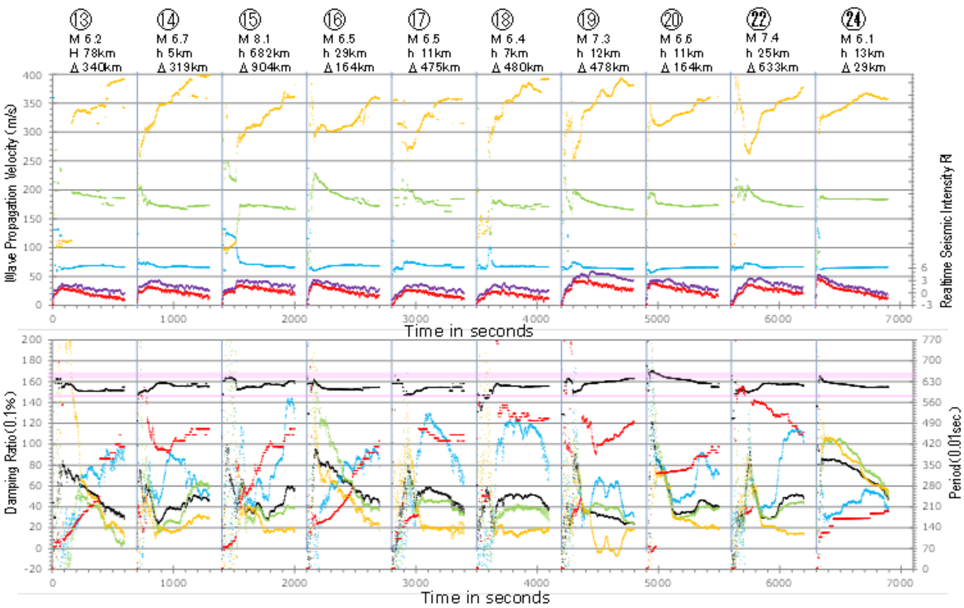

(d) Y(NS) Component with Oil Damper

Fig. 4(c)(d) – Results of the travel time analysis after the damper installation; change of the dynamic characteristics of the SKS building

At first, the natural period and damping factor for this building is considered with time variation or the other variations against input seismic intensity or input period.

(1) Time variation

At the time of the 311 Earthquake, the natural period of the X direction was enlarged to 7.03 seconds from about 6.2 seconds as the initial natural period by a motion exciter test and that of the Y direction was enlarged to 6.58 seconds from about 5.8 seconds as the initial natural period. Each of them increased almost 13 % longer than the initial natural period and then recovered gradually after the earthquake. As mentioned above, although the natural period of this building changes against each earthquake, the lower limit was mostly the initially measured natural period in case of both the X and Y directions before the installation of the anti-seismic devices. On the other hand, after the installation, the behavior of the Y direction suggests there is no change of stiffness because the natural period exists at the similar range. However the stiffness of the X direction becomes higher because the natural period became almost lower than the initially measured natural period. Thus, it is confirmed that although the oil damper gives no affect for stiffness, the steel damper improves the stiffness.

Next, the change of the damping factor among whole the building is considered. On the X direction, what the damping factor had been about over 4 % before the 311 Earthquake decreased drastically to about 1.5 % at the time of the event. Although it had recovered after that, it decreased again with the aftershock 30 minutes later. It recovered near 3 % at the time of the event in the next day, but it recovered only about 4 % at the time of the aftershock in July, 4 months later. After the installation of the steel damper, the damping factor of the X direction was around 4 – 6 % until the Kumamoto earthquake main shock. It was slightly larger value than that before the 311 Earthquake, and the Kumamoto earthquake main shock caused resonance with decreasing drastically near 1 %. After that, the damping factor recovered and varied between 2 – 6 %. The damping factor of Y direction had been 2 – 4 % before the 311 Earthquake. At the time of the 311 Earthquake, this building was trapped in resonant condition with drastically decreasing of the damping factor of less than 1 %, and the damping factor kept less than 1 % at least for 4 days after that event. Although it recovered over 2 % in case of the earthquake on April 7, 2011, it became less than 1 % again by the earthquake on April 11. Then it recovered over 2 % at the event more than four months later. After the installation of the oil dampers, although the damping factor decreased near 2 % by the Kumamoto earthquake main shock, it varies generally around 4 % and resonance was not caused.

(2) Variation against input seismic intensity or period

Fig. 5 shows the relationship between the natural period or the damping factor of this building and the input seismic intensity or period before and after the installation of the anti-seismic devices.

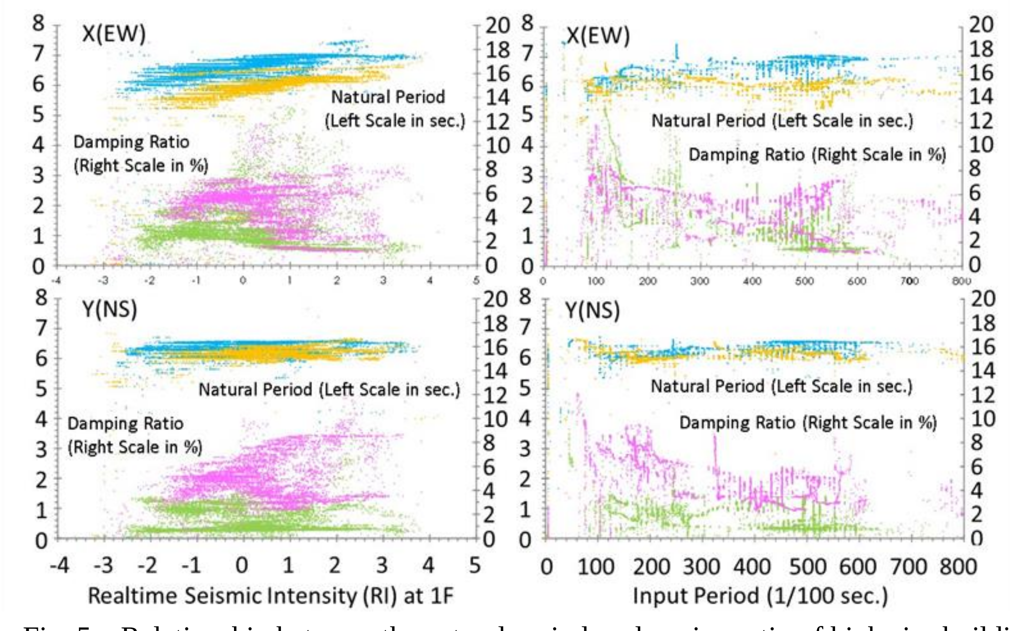

Fig. 5 – Relationship between the natural period or damping ratio of high-rise building SKS and RI at 1F (left side) or input period (right side): blue and green dots indicate the results without damper, orange and pink dots indicate the results with damper

While it is confirmed that the natural period of the X direction before the installation tends to increase with the input seismic intensity or period, that of the Y direction is almost constant against the input seismic intensity or period. The damping factor of the X direction is larger than that of the Y direction, and it is consistent with occurrence of resonance in the Y direction at the time of the 311 Earthquake during longer time than the X direction. The damping factor of the Y direction is mostly distributed less than 4 % and tends to decrease as input seismic intensity, but not clear. On the other hand, it is obvious that the damping factor of both the X and Y directions tends to decrease with increasing of the input seismic intensity.

The natural period of the X direction after the installation of the steel dampers shows a tendency to increase against the input seismic intensity as before the installation, but it is almost constant against the input period. That of the Y direction is almost constant against the input seismic intensity and also constant against the input period while becomes a little longer at less than 1.5 seconds. The damping factor is almost distributed less than 8 % for both the X and Y directions and there are both case as increasing and decreasing against the input seismic intensity. It generally decreases against the input period. While it is more than 2 % for the Y direction with the oil dampers, it becomes below 2 % for the X direction with steel dampers against the long period input motion. It is noticed as a relationship to occurrence of resonance at the X direction at the time of the Kumamoto earthquake main shock.

5.3 Behavior of the wave propagation velocity and the amplification factor for each section

(1) General

Fig. 4 shows that the wave propagation velocity at the section C has little variation and stable even during earthquake motion. So the member at the section C seems to keep the liner response against the events for this analysis. The wave propagation velocity at the section B has relative large variation and fluctuates relative largely during earthquake motion. Contrary to them, the wave propagation velocity at the section A has large variation and fluctuates largely during earthquake motion. Additionally the drift angle at the section A becomes large and seems to behave as non-linear response. On the damping factor, each section shows large variation against each event and behaves largely during earthquake motion.

Although the damping factor of the X direction before installation of the steel dampers has large variation, it distributed generally 4 % for the section A, 0 – 4 % for the section B, 6 – 10 % for the section C and totally around 4 % against the event #1. After the event #2 (the 311 Earthquake), it drastically decreased and became 2 – 4 % for the section A, minus value for the section B, 3 – 4 % for the section C and totally less than 2 %. After the event #4, it recovered gradually and it became around 2 % for the section A, 0 – 2 % for the section B, 3 – 4 % for the section C and totally about 2 – 4 %. Finally it had recovered the condition before the 311 Earthquake at the time of the event #10, about five months later. The damping factor of the Y direction became 0 – 2 % for the sections A and B, 6 – 9 % for the section C and totally 2 – 4 %. And then at the time of the event #2, it decreased drastically and became less than 1 % for the sections A and B and 2 % for the section C and got into a situation of resonance with totally falling down below 1 %. Then this situation continued and apparently once recovered when the event #6, but the damping factor decreased again at the time of the event #7 and recovered finally the condition before the 311 Earthquake at the time of the event #10, about five months later.

On the X direction after the installation of the steel dampers, the damping factor drastically decreased to less than 2 % for all the sections and totally around 1.5 % and got into a situation of resonance at the time of the event #19, the Kumamoto earthquake main shock. At the time of the other event, it was 0 – 1 % for the section A, 2 – 7 % for the section B, widely scattering as around 12 % for the section C and totally around 4 – 6 %. On the Y direction, although the damping factor had large scatter but totally not less than 2 %, and it kept over 2 % for the section A, over 4 % for the section B and over 3 % for the section C without at the time of the event #19. In case of the event #19, the damping factor kept totally over 2 % without partially 0 % for the section A, and the situation of resonance was not occurred at the Y direction with oil dampers.

(2) Anisotropy and other characteristics of the wave propagation velocity for each section

The wave propagation velocities of the each section differ from each direction and the anisotropy is clearly recognized. That of the section C is lower than 100 m/s for each direction, and the rigidity of the Y direction weakened as the wave propagation velocity was around 90 m/sec for the X direction and around 65 m/sec for the Y direction. The wave velocity of the section B is around 150 m/sec and the rigidity of the Y section direction is rather high. On the other hand, the section A shows quite different characteristics. At the section A, the wave propagation velocity of the X direction is estimated about 200 m/sec but it decreased to about 170 m/sec by the large earthquake motion by the 311 Earthquake, event #2. It showed a tendency to recover, but it decreased more by the event #3. It also recovered when the event #4, but the result of the calculation is unstable at the later part because it might be too small amplitude. On the other hand, the wave propagation velocity of the Y direction shows anomalous characteristics as great fluctuations between each event or even during individual event. As Fig. 1, this building broadens towards the bottom from 8F to 1F at the Y direction of the section A for reducing the ground contact pressure, and this portion has high rigidity. It is considered that this structure caused the complicated behavior of the wave propagation velocity at the Y direction of the section A.

(3) Behavior against input seismic intensity and period

Next, the behavior of the wave propagation velocity and the damping factor of each section are considered with the input seismic intensity and period. Fig. 6 shows the result before and after the installation of the anti-seismic devices for each direction.

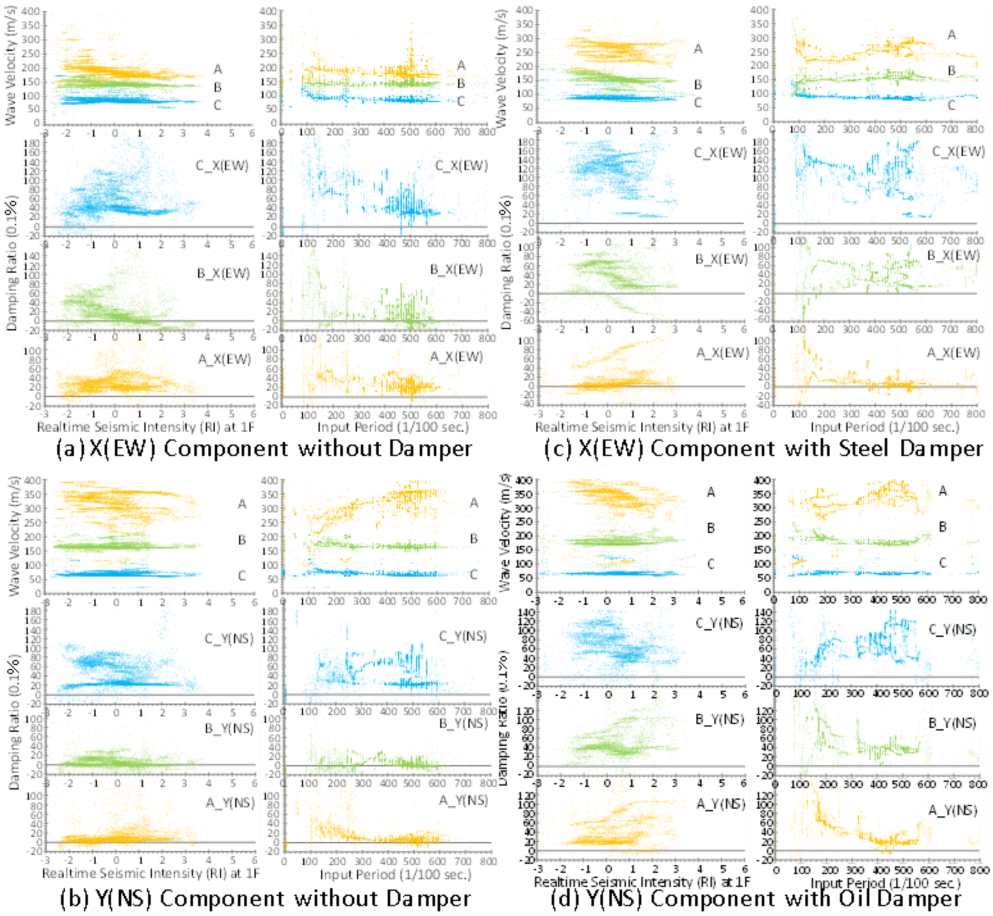

Fig. 6 – Relationship between the wave propagation velocity or the damping ratio and RI at 1F or the input period

On the wave propagation velocity of the X direction before the installation, that of the sections A and B tends to decrease when large input seismic intensity or long input period but there is little change in that of the section C. Whereas, that of the Y direction is nearly stable at the sections B and C against both the input seismic intensity and period, but there seems to be two cases as clearly decreasing of the wave propagation velocity and decreasing not so largely against the input seismic intensity. Against the input period, the wave propagation velocity of the section A obviously shows the tendency to become large with elongating of the input period. It is estimated that this relates to the structure broadening towards the bottom at the section A.

After the installation of the anti-seismic devices, the wave propagation velocity of the X direction obviously becomes large at the sections A and B as comparing with that before the installation. And it is confirmed not only the behavior the wave propagation velocity decreases with increasing the input seismic intensity as seen before the installation but also the case not decreasing at the section A. Additionally, a phenomenon decreasing the wave propagation velocity with lengthening the input period can be recognized both at the sections A and B, and it is noticeable at the section A with a lot of steel dampers. Because this phenomenon is similar to the situation at the Y direction of the section A before the installation of the dampers, it is considered to be caused by the effect of the reinforcement by the steel dampers. On the wave propagation velocity of the Y direction, although there is no significant variation at the section C, that of the sections A and B seems to become slightly larger. For the Y direction, oil dampers were installed at the sections A and B, and it may cause a slight increasing of the rigidity.

Considering the damping factor, although that of the X direction was obviously larger than that of the Y direction before installation of the anti-seismic devices, that becomes almost similar value for each direction after the installation. In more detail, the damping factor of the X direction at the section C became large even without the anti-seismic devices after the installation of them for the sections A and B, but it is considered that the damping factor becomes apparently large because what the damping factor had become totally small by the affection of the 311 Earthquake before the installation of these devices returned to its former state. It is noteworthy for the damping factor of the X direction at the section C with the long period input wave that there is a group of smaller damping factor under 2 %, at the time of the Kumamoto earthquake main shock, than that before the installation of the anti-seismic devices.

On the X direction, the damping factor at the section A with the steel dampers tends to become large with enlargement of the input seismic intensity. The number of the steel dampers at the section B is one fifth less than that at the section A, and the damping factor at the section B basically decreases with increasing input seismic intensity. Although there was no significant change on the damping factor at the sections A and B against the short period input less than 2 seconds both before and after the installation of the steel dampers, that against the long period input around 5 seconds obviously decreased after the installation of them. It is to be noticed that the damping factor decreases and becomes minus against short period input or that against long period input becomes smaller than that before the installation of the steel dampers. The latter requires more detailed consideration with the relationship to the resonance with drastically decreasing of the damping at the Y direction during the 311 Earthquake.

Next, the damping at the Y direction is considered. There is a data group of small damping factor as 0 – 2 % for each section seemed to be caused by the 311 Earthquake before installation of the anti-seismic devices. Additionally, it is confirmed that there is also a data group around 2 – 10 % at the section C. The damping factor of the section C basically tends to increase against the input period before and after the installation of the oil dampers without the damping factor around 2 % might be caused by the 311 Earthquake. The damping factor of the sections A and B roughly shows a tendency to increase after the installation with increasing the input seismic intensity, and it is considered that there is an under limit of the damping factor although the damping factor shows a tendency to obviously decrease with increasing input period. In any case, the damping factor becomes obviously larger than that before the installation of the oil dampers.

6. Discussion

6.1 Summary on the effect of the anti-seismic devices

The effect of the anti-seismic devices can be summarized as follows.

On the X direction, the wave propagation velocity associated with the rigidity becomes large for both the sections A and B after the installation of the steel dampers. It becomes larger with increasing the input period and reaches the peak at around 5 seconds. It is remarkable especially at the section A. The damping factor after the installation of the steel dampers decreased both at the sections A and B and becomes less than around 1 % especially against the input period around 5 – 6 seconds. This means that the steel damper works to improve the rigidity but does not contribute the improvement of the damping, against long period input.

On the Y direction, the wave propagation velocity associated with the rigidity has almost no change without slight increase both at the sections A and B after installation of the oil dampers. And the damping factor decreases clearly against increasing the input period, but it increases farther than that before the installation. Especially in case of input period around 5 seconds, the damping factor increases to 2 % for the section A or 4 % for the section B from almost 0 %.

It is necessary to continue considering whether the drastic decreasing is common characteristics of steel structures or whether the anti-seismic devices can cover this phenomenon.

6.2 On the resonance

Resonance phenomenon can be confirmed at the time of the 311 Earthquake main shock, event #2, its aftershock, event #3 and the Kumamoto earthquake main shock, event #19. Fig. 7 is a comparative diagram between the accelerogram of the X and Y directions and the behavior of the natural period of this building, the period of the input earthquake motion or the damping factor of this building, for each event.

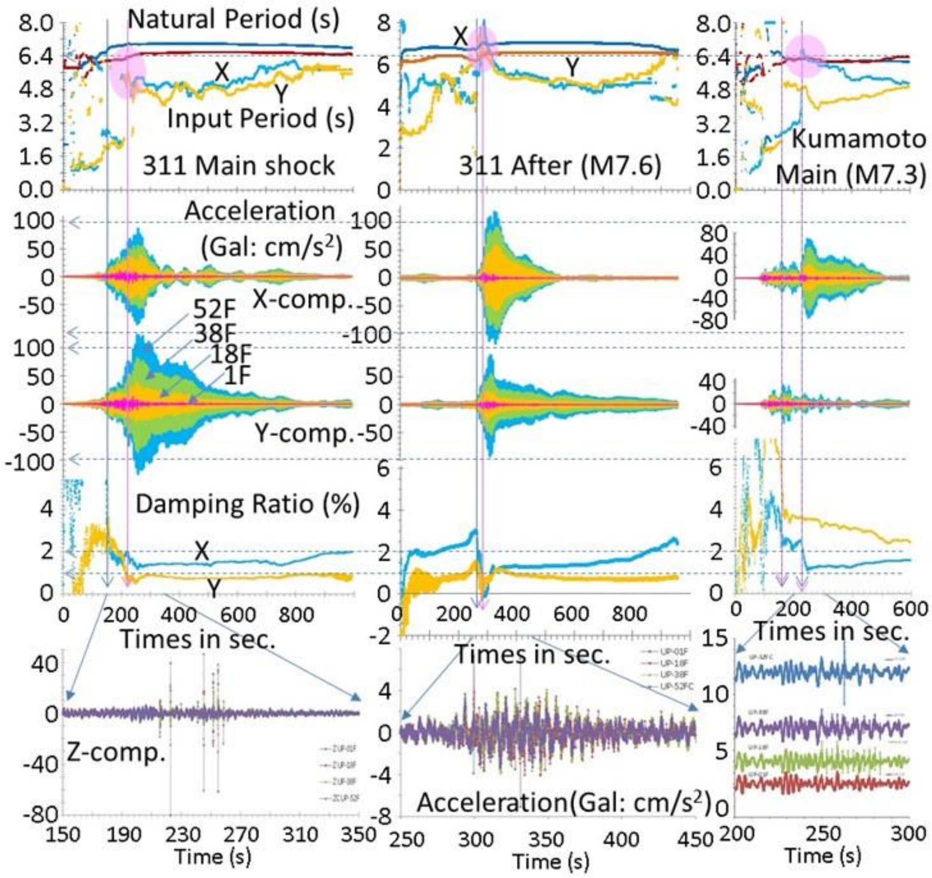

Fig. 7 – Resonance situation for three earthquakes; main shock and aftershock of the 311 Earthquake and the Kumamoto earthquake: relationship with the input period, natural period, damping ratio, waveforms and so on

Fig. 7 indicates that the drastic decreasing of the damping occurred almost coincidentally with the starting resonance of this building. In case of the X and Y direction of the 311 Earthquake aftershock, event #3, and the X direction of the Kumamoto earthquake main shock, event #19, the resonance started when the natural period of this building and input period approximately coincided.

It is notable that the amplification of the seismic intensity at the section A became exceptionally large at that time. At the time of the 311 Earthquake, the input period of the Y direction got closer to near 90 % of the natural period of this building, and the resonance situation was caused coupling with decreasing the damping. On the other hand, the natural period of this building was lager at the X direction before the installation of the steel dampers and was over 6.4 seconds as the dashed line for each direction, but it became similar value for each direction less than 6.4 seconds after the installation. It means that the stiffness of this building increased after the installation of the steel dampers.

On the damping factor after drastic decreasing, that of the X direction is similar value for these three events within a range between 1 % as a dashed line and 2 % as the other dashed line. On the other hand, which that of the Y direction was less than 1 % before installation became almost more than 3 % after the installation. It is considered from these figures that the necessary requirement to get into a resonance situation is to become lower than about 1.5 % of the drastic decreasing damping factor. And then, the drastically decreased damping factor by the 311 Earthquake or the Kumamoto earthquake main shock had gradually recovered and finally returned to the original value about half year later.

Additionally, pulse waves are overlapped on the vertical motion waveforms for these events around the time of occurrence the resonance. It is considered that there is an interrelation between the natural period of this building, the period of input earthquake motion, decreasing of the damping factor, the resonance phenomenon, the pulse wave and so on. So it is interesting that these items relate to the condition of the occurrence of the resonance. Especially, it is necessary to continuously follow the behavior of the dampers against input of the long period motion.

7. Conclusion

This paper confirmed how the wave propagation velocity and the damping factor of the SKS building change during the earthquake motion using the CERS methods to understand in realtime how the physical property of buildings or ground changes during earthquake motion or normal situation. The anti-seismic devices have been additionally installed for the SKS building as a countermeasure for the earthquake disasters. And this paper obtained interesting results as capturing the changing situation of the physical properties with the devices. The resonance of buildings relates to the natural period and the amplification or damping characteristics of the building and input period and amplitude. It is considered that defining the condition causing resonance may construct proper countermeasures to mitigate the resonance. The author would like to keep considering from this viewpoint with further detailed analysis in the future.

8. Acknowledgement

Strong motion records were provided by Building Research Institute. The author thanks deeply for Dr. Toshihide Kashima and other concerned personnel.

9. References

[1] Yutaka Nakamura: On the CERS methods, realtime assessment methods for a travel time and a damping (in Japanese), Proceedings of JAEE annual meeting, P4-20, December. 2017.

[2] Yutaka Nakamura: On the CERS methods for realtime evaluation on a travel time and damping, under submitting to 17 WCEE, Sendai, JAPAN, September. 2020.

[3] Tsutomu Sato, Yutaka Nakamura and Jun Saita: Non-linier Analysis for Ground of Port Island using CERS methods (in Japanese), Proceedings of JAEE annual meeting, P4-21, December. 2017.

[4] Osaka Prefecture: Implementation status of long-period ground motion countermeasure construction (in Japanese), http://www.pref.osaka.lg.jp/otemaemachi/saseibi/taisaku-jyokyo.html, last updated 2018.5.22.

[5] Yutaka Nakamura: Examination of a rational strong motion index - Relationship between the DI value and the other strong motion indices - (in Japanese), Proceedings of the 27th JSCE Earthquake Engineering Symposium, Japan Society of Civil Engineers, December. 2003.

